

# Why does my medical AI look at pictures of birds? Exploring the efficacy of transfer learning across domain boundaries

**Frederic Jonske**<sup>1</sup>, Moon Kim<sup>1</sup>, Enrico Nasca<sup>1</sup>, Janis Evers<sup>1</sup>, Johannes Haubold<sup>2</sup>, René Hosch<sup>1,2</sup>, Felix Nensa<sup>1,2</sup>, Michael Kamp<sup>1,3,4</sup>, Constantin Seibold<sup>1</sup>, Jan Egger<sup>1,5</sup>, Jens Kleesiek<sup>1,5,6</sup>

{**frederic.jonske**, moon-sung.kim, enrico.nasca, johannes.haubold, rene.hosch, felix.nensa, michael.kamp, constantin.seibold, jan.egger, jens.kleesiek}@uk-essen.de  
janis.evers@stud.uni-due.de

1 - Institute of AI in Medicine (IKIM), University Medicine Essen (AöR), University Duisburg-Essen, Germany

2 - Institute of Diagnostic and Interventional Radiology and Neuroradiology,  
University Medicine Essen (AöR), Germany

3 - Institute for Neuroinformatics, Ruhr University Bochum, Germany

4 - Department of Data Science & AI, Monash University, Australia

5 - Cancer Research Center Cologne Essen (CCCE), University Medicine Essen (AöR), Germany

6 - Department of Physics, TU Dortmund University, Dortmund, Germany

## **Abstract**

It is an open secret that ImageNet is treated as the panacea of pretraining. Particularly in medical machine learning, models not trained from scratch are often finetuned based on ImageNet-pretrained models. We posit that pretraining on data from the domain of the downstream task should almost always be preferred instead.

We leverage RadNet-12M, a dataset containing more than 12 million computed tomography (CT) image slices, to explore the efficacy of self-supervised pretraining on medical and natural images. Our experiments cover intra- and cross-domain transfer scenarios, varying data scales, finetuning vs. linear evaluation, and feature space analysis.

We observe that intra-domain transfer compares favorably to cross-domain transfer, achieving comparable or improved performance (0.44% - 2.07% performance increase using RadNet pretraining, depending on the experiment) and demonstrate the existence of a domain boundary-related generalization gap and domain-specific learned features.

## **1 Introduction**

Is there a guaranteed-to-be-best dataset to pretrain on, given a task? One could argue that any task's dataset is best represented by features learned on itself or a dataset from the same underlying distribution or domain. This representativeness is something other datasets cannot necessarily guarantee. More specifically, we ask: "Why is my medical AI looking at pictures of birds? Should it not look at pictures of tumors to learn about tumors?" On the other hand, one could argue that any image should be representable by a generic set of features, no matter where that set is learned, just like a human could describe a previously unseen image accurately, using only a small number of words. After all, humans are also "pretrained" on

natural images while growing up, before “getting finetuned” on medical images to become radiologists.

In the literature, many papers describe successful transfer learning applications where pretraining on one domain improves finetuning on another, while others found that unsupervised pretraining offered no substantial improvements, implying both lines of reasoning have at least some merit:

Cherti & Jitsev [1] explored the efficacy of supervised pretraining and transfer learning in medical-medical, natural-natural and cross-domain scenarios. Their findings indicated that in some cases, upscaling the available pretraining data led to proportionally increased performance, while for few-shot tasks the effect disappeared. They additionally reported that models pretrained on ImageNet-21k [2] outperformed models pretrained on the largest available X-Ray datasets when finetuning on X-Ray image downstream tasks. Notably, the combined number of labeled X-Rays available for this comparison were about 16 times fewer than the images contained in ImageNet-21k (approx. 873k vs. approx. 14M).

Leveraging around 100 million medical images from multiple modalities for self-supervised pretraining, Ghesu et al. reported that their self-supervised algorithm, together with the significant dataset upscaling, yielded a significant advantage over both training from scratch and pretraining with other methods, achieving state-of-the-art performance across several medical downstream tasks [3].

Mei et al. created RadImageNet, a dataset composed of 1.4 million medical images and reported that models trained on RadImageNet achieved superior performance compared to ImageNet-pretrained models [4]. Their downstream tasks consisted of medical images. They further observed a correlation between the size of the dataset in the downstream task and the transfer learning performance, noting that RadImageNet yielded greater improvements on smaller datasets.

While noting that ImageNet-pretraining was often a *de facto* method for medical image classification problems, Raghu et al. observed across a range of different model architectures and medical imaging tasks, that pretraining with ImageNet yielded no significant performance boost and that meaningful feature reuse did not always occur after pretraining [5].

Newell & Deng [6] experimentally probed the efficacy of self-supervised training using synthetic data and various pretraining algorithms. They observed an anti-proportional correlation between pretraining utility and the number finetuning images and noted that in some cases, pretraining offered only accelerated convergence or even no performance gain. In a study on cross-domain generalization [7], which pretrained on publicly available data, Cohen et al. found that many of their models could perform well after finetuning on the same downstream task, yet disagree in their predictions, as well as that models that were in strong agreement nonetheless performed poorly, implying that generalization to other tasks is often a nuanced process.

A study by Gururangan et al. [8] explored intra-domain transfer learning on Natural Language Processing (NLP) tasks, using multi-phased pretraining on different datasets. They found that spending at least some time training on data from the domain of the downstream task led to consistent performance gains.

Based on these previous findings and the lines of reasoning we offered above, we formulate the following hypotheses:

1) When applying transfer learning, any difference between the pretraining and finetuning task domains produces a *generalization gap* [9]. This happens because the two underlying data

distributions, and consequently learned feature subsets, are likely to be different at least to some degree [10], [11]. Intuitively, we expect this gap to shrink or disappear in an intra-domain transfer learning scenario, since the data distributions are highly similar or identical. In essence, we propose that **“there is no better data to train medical questions on than medical data”**.

II) The generalization gap effect is not symmetrical. A model trained on a specific pretraining dataset may learn a superset of the features or concepts it would learn from a different dataset. While this is most likely not true for every downstream task at once (because that would require the training dataset to be representative for every such task), it may well be true for a significant fraction of them. We posit that **“some pretraining datasets are principally more useful than others”**.

Providing an answer to which of these two hypotheses is true not only provides fundamental insights into the nature of finetuning and domain adaptation and transfer learning, but more importantly provides us with practical strategies to improve our medical AI models.

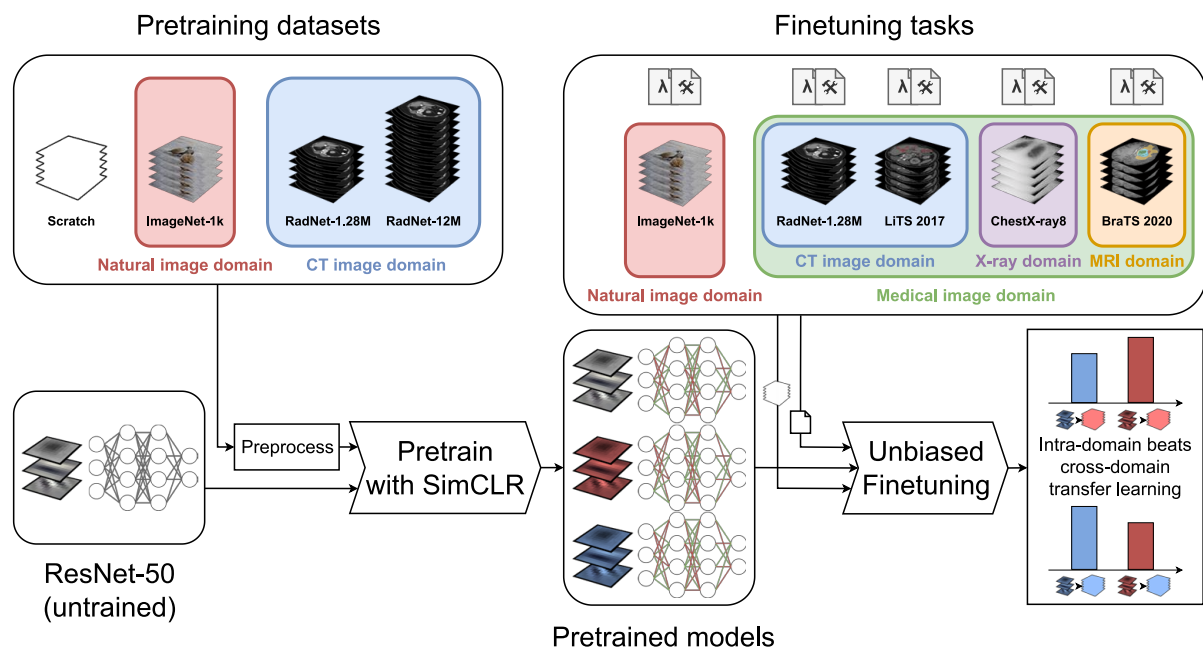


**Fig. 1: Schematic visualization of the transfer learning experiment.**

During the transfer learning experiment, models are pretrained on medical, natural, or no images and the value of the pretraining in terms of performance gains is measured across a number of downstream tasks, which also come from the medical or natural image domain. Each downstream task has a set of hyperparameters and build instructions that is shared between executions and makes extension of the framework straightforward and more easily reproducible.

Our main contributions are as follows:

- To validate these hypotheses, we leverage RadNet-1.28M and RadNet-12M, two pretraining datasets comprised of 12 million CT image slices from our local hospital and four publicly available datasets from the natural and medical image domain.
- We design an experimental setup (cf. Fig. 1 and the Methods section) to compare unsupervised pretraining efficacy, depending on dataset domain, task complexity, and in a linear evaluation vs finetuning scenario.
- We present our results and uncertainty estimations, discuss them with respect to our hypotheses, and perform feature space analysis for our models.

- Finally, we discuss guidelines for the choice of pretraining datasets, depending on downstream tasks, and publish our code framework and pretrained models for the reproduction or extension of our work.

## **2 Methods**

### **2.1 Datasets and tasks**

#### **2.1.1 RadNet-X**

The RadNet-X datasets were created specifically for the purpose of this work. The computed tomography (CT) data stems from the PACS of the University Hospital Essen, Germany, and was tested for eligibility in the following manner: Every image with fewer than 30 slices in the z-direction is excluded to guarantee that data comes from high resolution scans and to guarantee exclusion of things like screen captures, scouts, or topograms. Every image slice with fewer than 25% coverage (anything other than air) is also removed. Every remaining slice is resampled to 256 x 256 pixels in size. There are no additional exclusion criteria based on patients or dates. This process yielded 12,034,617 slices (approx. 84.8% the size of ImageNet-21k) from 90,663 CTs. Data used by Koitka et al. [15] and Jonske et al. [16] was reused for this study. We opt for only a single modality because we intend to test our hypotheses on a narrow, clearly defined subdomain. The slices are automatically labeled based on metadata, dividing them into 7 anatomical classes – “head”, “thorax”, “abdomen”, “extremities”, “pelvis”, “spine”, and “other”.

Since comparability with ImageNet-1k is the stated goal of this dataset, the RadNet-1.28M dataset contains exactly as many slices as ImageNet-1k does images, while the RadNet-12M dataset contains every slice available. RadNet-1.28M maintains the same ratio of classes as RadNet-12M, but excludes images of the “other” class (which includes slices impossible to label, such as those belonging to whole-body images, for which every slice would belong to the “other” class). RadNet-1.28M is used as a pretraining and finetuning (classification) dataset, while RadNet-12M is only used as a pretraining dataset.

Due to human anatomy, there exists a strong correlation between neighboring slices of every CT image. This correlation effectively reduces the amount of information contained in the dataset compared to one in which every image slice comes from a different scan. In the Results section, we report results for RadNet-1.28M LB (lower bound) and UB (upper bound). These results are interpolated using RadNet-1.28M, RadNet-12M, and a scale factor (see supplementary materials), to offset this effect. We note that when comparisons are drawn between ImageNet and RadNet, we generally refer to RadNet-1.28M (LB/UB-adjusted), as RadNet-1.28M and RadNet-12M themselves do not offer a fair comparison to ImageNet-1k in terms of image numbers. As discussed in the supplementary materials, we consider RadNet-1.28M (UB-adjusted) results the closest radiological imaging analog to ImageNet-1k.

While we cannot make the dataset itself publicly available, the pretrained model weights for both RadNet-X datasets are made publicly available (permission granted by the responsible IRB, cn. 20-9745-BO).

### **2.1.2 ImageNet-1k**

ImageNet-1k [2] consists of 1.28 million RGB images of 1000 classes. Human-created labels exist for every point of data and have a one-to-one relation with images. We perform pretraining and finetuning on this dataset. We make an even, stratified split of the official validation set to obtain a validation and test set.

### **2.1.3 LiTS 2017**

LiTS (Liver Tumor Segmentation) 2017 [12] is a segmentation dataset composed of abdominal CT images. The data comes from 131 distinct patients and totals 41'561 individual 2D slices, all of which are professionally segmented into background, liver, and tumor regions. We use LiTS only as a downstream segmentation task. The official validation set is evenly split to obtain a validation and test set.

### **2.1.4 BraTS 2020**

BraTS (Brain Tumor Segmentation) 2020 [13] is a segmentation dataset composed of cranial MRT scans. The training data comes from 369 glioma patients. For each patient, T1, T1ce, T2, and FLAIR modalities are available. Tumor regions are divided into Tumor Core (TC), Active Tumor (AT), and Whole Tumor (WT) regions. BraTS 2020 is used only as a downstream segmentation task. Empty slices are removed from the dataset. We use 30 patients each from the official training dataset to construct a validation and test set.

### **2.1.5 ChestX-Ray8**

ChestX-Ray8 [14] is a medical imaging dataset containing 108,948 frontal-view X-ray images of 32,717 unique patients. Classification labels for each X-ray were automatically acquired by text-mining the corresponding reports for specific disease symptoms. As the dataset contains instances with multiple findings, we use ChestX-Ray8 as a downstream classification task but extend the cross-entropy loss to cover multi-label cases. We construct a training and validation set from the official "train\_val" set using a 90-10 split. Due to the multi-label classification, these subsets are not stratified. To avoid bias from an uneven split, these subsets (but not the test set) are randomized between multiple runs of the same experiment.

## **2.2 Experimental setup**

To test our hypotheses, we combine all four pretraining options (training from scratch, ImageNet-1k, RadNet-1.28M, and RadNet-12M) and all five finetuning tasks (ImageNet classification, RadNet classification, ChestX-Ray8 multi-label classification, LiTS 2017 segmentation, and BraTS 2020 segmentation) in several different settings.

To pretrain, we apply the self-supervised contrastive algorithm SimCLR [17] on a ResNet-50 [18] architecture. We choose self-supervision during pretraining to circumvent the annotation bottleneck of medical imaging datasets. The ResNets are randomly initialized. Pretraining is performed with a batch size of 4096, using the LARS optimizer [19]. For the learning rate, we apply the square root rule used by Chen et al. [17], yielding a learning rate of 4.8. All input images are resized to 3 x 256 x 256 pixels so that all models possess the same number of

parameters, facilitating fair comparison between the datasets. For RadNet images this is done by concatenating the same slice thrice along the channel axis. All images are normalized to the range [0, 1]. All models are pretrained on their respective datasets for 100 epochs, using NT-CrossEntropy Loss [17]. To prevent pretraining instability from information leakage, our ResNet-50 uses SyncBatchNorm [20] in place of BatchNorm [21].

For the finetuning, the SimCLR MLP head is replaced by a new head. To use the pretrained models, RadNet, LiTS 2017 and ChestX-Ray8 images are converted to three-channel images as described above. For BraTS 2020, the T2 channel is discarded for the same reason (discarding the T2-channel empirically had the smallest performance impact). Finetuning is performed with a common set of hyperparameters per individual finetuning task, regardless of the pretraining dataset, to allow for a fair comparison (for a detailed discussion on this matter, refer to the supplementary materials). Where necessary for segmentation, we extend the ResNets into a symmetrical U-Net-like [22] architecture. Newly added parts of a model are randomly initialized with PyTorch [23] default settings. All loss functions used are CrossEntropyLoss or a variation thereof (pixel-wise cross entropy for segmentations, multi-label cross entropy for ChestX-Ray8). For specific hyperparameters or further implementation details, consult the supplementary materials or our code and documentation (<https://github.com/TIO-IKIM/Transfer-learning-across-domain-boundaries>)

## **2.3 Initial Experiments**

### **2.3.1 Experiment 1 (Task Dependency)**

According to hypothesis 1, we expect to see a generalization gap when the pretraining and finetuning dataset domain are different. If hypothesis 1 is correct, we expect RadNet-pretrained models to outperform ImageNet-pretrained models on the RadNet and potentially ChestX-Ray8, BraTS 2020, and LiTS 2017 downstream tasks. Simultaneously, we test hypothesis 2 - if the relative performance loss in the cross-domain transfer scenarios is asymmetrical, this is a strong indication that hypothesis 2 is correct.

### **2.3.2 Experiment 2 (Finetuning vs. Linear Evaluation)**

To investigate hypothesis 2 further, we perform a linear evaluation by allowing only a single learnable linear layer on top of the otherwise frozen pretrained models. This effectively increases the difficulty of the task and enforces the reuse of features learned during pretraining. For segmentation tasks, the added U-Net decoder is necessarily randomly initialized at the start of the linear evaluation and thus needs to be trained to achieve any meaningful results. In this case, we allow the training of weights of half the model.

### **2.3.3 Experiment 3 (Task Complexity)**

In a few-shot transfer learning scenario, features learned during pretraining in the same domain should, intuitively, be significantly more useful than those learned in a different domain. Few-shot finetuning allows for very little change in feature compositions, simply because there are fewer overall training steps. Indeed, a similar effect has been observed by Cherti & Jitsev [1]. We define the complexity of a task as the ratio of labeled examples per number of target classes. We increase this complexity by decreasing the training dataset size to 50% (M), 10% (S), 1% (XS), or 0.1% (XXS) in a stratified manner, or decrease it by removing classes. The original task's validation and test sets are kept.

## 2.4 Reported metrics

For classification tasks, we report the accuracy (ImageNet, RadNet) and average AUC (ChestX-Ray8), while for segmentation tasks (LiTS 2017, BraTS 2020) we report DICE scores for each class. We also provide uncertainty estimates for all metrics, based on four separate runs of the same experiment (using the same hyperparameters and dataset splits, but different random initializations). Finally, we report relative performance comparisons and their significance based on Welch’s t-test [24] (cf. “S1 - Significance of experimental results” in the supplementary materials).

## 3 Results

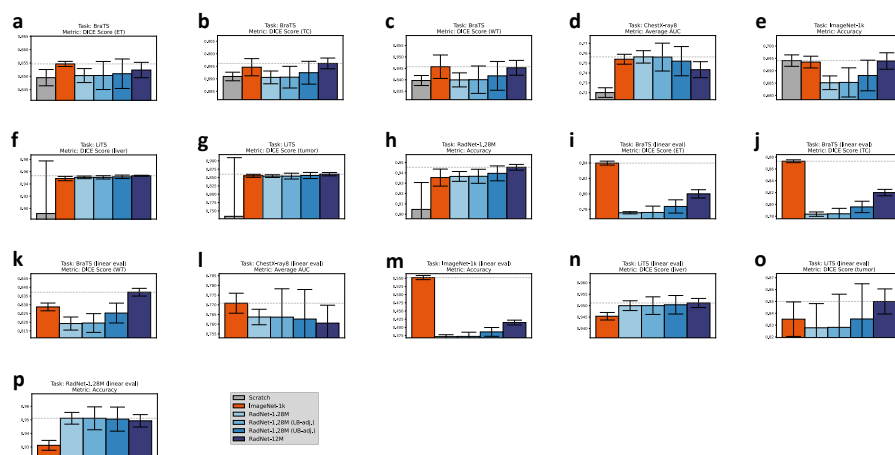


**Fig. 2: Intra-domain outperforms cross-domain transfer learning.**

Performance across four separate runs for every combination of pretraining dataset and finetuning task of experiments 1 and 2 are on display: **a**, Finetuning on BraTS 2020 (Enhancing Tumor). **b**, Finetuning on BraTS 2020 (Tumor Core). **c**, Finetuning on BraTS 2020 (Whole Tumor). **d**, Finetuning on ChestX-Ray8. **e**, Finetuning on ImageNet-1k. **f**, Finetuning on LiTS 2017 (Liver). **g**, Finetuning on LiTS 2017 (Lesion). **h**, Finetuning on RadNet-1.28M. **i**, Linear evaluation on BraTS 2020 (Enhancing Tumor). **j**, Linear evaluation on BraTS 2020 (Tumor Core). **k**, Linear evaluation on BraTS 2020 (Whole Tumor). **l**, Linear evaluation on ChestX-Ray8. **m**, Linear evaluation on ImageNet-1k. **n**, Linear evaluation on LiTS 2017 (Liver). **o**, Linear evaluation on LiTS 2017 (Lesion). **p**, Linear evaluation on RadNet-1.28M.

Firstly, we observe that pretraining on any dataset yields some degree of improved performance in almost every finetuning scenario we tested (cf. Figs. 2, 3). We further observe that intra-domain transfer learning (e.g. RadNet→RadNet) generally offers equal or slightly improved performance compared to cross-domain transfer learning (e.g. ImageNet→RadNet), although this is not unambiguously observed everywhere. If the complexity of the task is increased by reducing the number of images per class during finetuning, or only linear evaluation is performed instead of finetuning, this intra-domain advantage grows both in absolute terms (cf. Figs 2, 3) and in statistical significance.

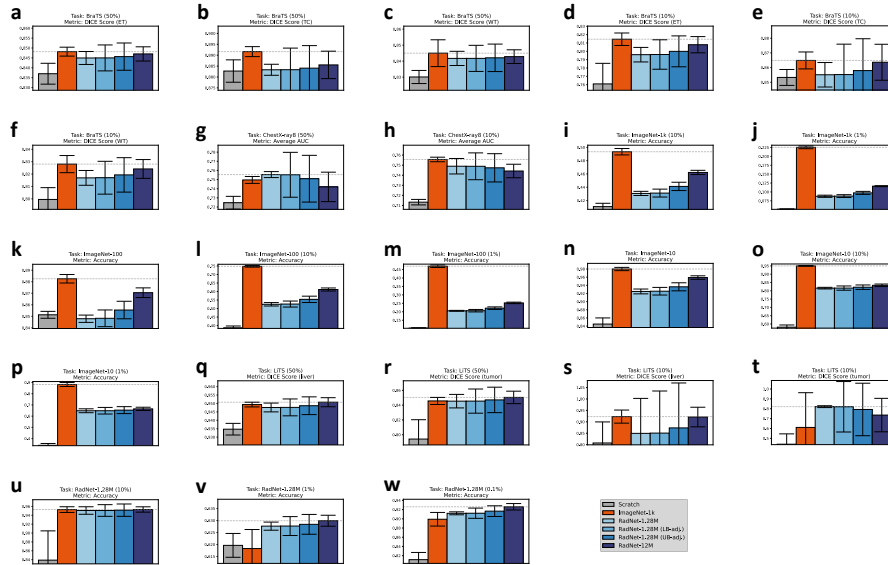


**Fig. 3: The intra-domain advantage scales with task complexity.**

Performance across four separate runs for every combination of pretraining dataset, finetuning task of experiment 3 are on display: **a**, Finetuning on BraTS 2020 (50%, Enhancing Tumor). **b**, Finetuning on BraTS 2020 (50%, Tumor Core). **c**, Finetuning on BraTS 2020 (50%, Whole Tumor). **d**, Finetuning on BraTS 2020 (10%, Enhancing Tumor). **e**, Finetuning on BraTS 2020 (10%, Tumor Core). **f**, Finetuning on BraTS 2020 (10%, Whole Tumor). **g**, Finetuning on ChestX-Ray8 (50%). **h**, Finetuning on ChestX-Ray8 (10%). **i**, Finetuning on ImageNet-1k (10%). **j**, Finetuning on ImageNet-1k (1%). **k**, Finetuning on ImageNet-100. **l**, Finetuning on ImageNet-100 (10%). **m**, Finetuning on ImageNet-100 (1%). **n**, Finetuning on ImageNet-10. **o**, Finetuning on ImageNet-10 (10%). **p**, Finetuning on ImageNet-10 (1%). **q**, Finetuning on LiTS 2017 (50%, Liver). **r**, Finetuning on LiTS 2017 (50%, Lesion). **s**, Finetuning on LiTS 2017 (10%, Liver). **t**, Finetuning on LiTS 2017 (10%, Lesion). **u**, Finetuning on RadNet-1.28M (10%). **v**, Finetuning on RadNet-1.28M (1%). **w**, Finetuning on RadNet-1.28M (0.1%).

We further note that the observed intra-domain advantage is not symmetrical - for example, pretraining on RadNet instead of ImageNet, followed by linear evaluation on RadNet, offers a statistically less significant and substantially smaller relative performance gain than the reverse case ( $\Delta_{R-1.28M} = 0.44\%$ ,  $p = 0.541$  vs.  $\Delta_{I-1k} = 0.79\%$ ,  $p = 0.231$ ). This asymmetry appears to intensify during linear evaluation ( $\Delta_{R-1.28M}(\text{lineval}) = 2.07\%$ ,  $p = 0.025$  vs.  $\Delta_{I-1k}(\text{lineval}) = 42.92\%$ ,  $p < 0.001$ ) or for increasing task complexity ( $\Delta_{R-1.28M}(XXS) = 1.63\%$ ,  $p = 0.114$  vs.  $\Delta_{I-1k}(XS) = 131.62\%$ ,  $p < 0.001$ ).

Notably, the observed intra-domain advantage does not apply across all medical imaging tasks - RadNet-1.28M pretraining yields slightly superior or comparable performance only on RadNet and LiTS (both CT imaging datasets), but inferior performance on BraTS (an MRI dataset), for example.

Additionally, we note that even between target classes in the same task, different behaviors can be observed. For example, RadNet-pretrained models generally outperform ImageNet-pretrained models in liver segmentation, but not tumor segmentation, where RadNet-1.28M (UB-adjusted) performs similarly to ImageNet-1k. This effect is conserved when linearly evaluating, making it unlikely that the effect is purely a statistical coincidence.



## **4 Discussion**

From our above observations, we conclude that cross-domain transfer learning indeed degrades performance compared to intra-domain transfer learning in accordance with our first hypothesis, particularly in few-shot or linear evaluation scenarios. On CT-based downstream tasks (e.g. RadNet→RadNet vs. ImageNet→RadNet, cf. Fig. 2), the intra-domain advantage is relatively small and only observed with any statistical significance over many runs, compared to natural image-based tasks. We argue that there are multiple factors at play in such cases:

1. If a task is very simple, the finetuning process will likely “solve” it, irrespective of any pretraining or frozen weights, given enough time. As RadNet-1.28M only possesses 6 classes, compared to ImageNet’s 1,000, this appears probable. However, since finetuning from scratch still yields a lower performance than pretrained models, an additional explanation is needed.
2. In some cases, unstable training can obfuscate predicted effects through large uncertainties - this is particularly true for few-shot transfer scenarios, where overfitting can easily occur.

Our first explanation is corroborated by the loss behavior during training (cf. Fig. 4). Despite similar test-time performance, the train-time loss falls at markedly different speed between pretraining on medical or natural images (or nothing at all), meaning the intra-domain advantage, while probably extant, is strongly suppressed. This phenomenon may provide an explanation for the findings of Newell & Deng [6], who frequently observed no tangible performance gains for self-supervised pretraining, but often observed an initially accelerated increase in performance during training. Interestingly, while pretraining almost universally improved convergence speed, an intra-domain advantage is only observed in some experiments and is not statistically significant in many cases. Again, this effect is stronger for greater task complexity (cf. Fig 4). Our second explanation is substantiated by the fact that the expected intra-domain advantage for both data domains is visible and amplified substantially for most few-shot finetuning scenarios (see Results).

The asymmetrical generalization gap we observe follows an intuitive logic: Information encoded in the color channels has different meanings between RadNet- and ImageNet-pretraining - whereas models pretrained on ImageNet can reuse any texture-encoding feature and “discard” color-encoding features in a cross-domain transfer scenario, RadNet-pretrained models must learn an entirely new concept in the reverse case. The asymmetry and its dependency on task complexity corroborate our second hypothesis, that some pretraining datasets generalize better than others, as ImageNet pretraining delivers a set of features that on average transfer extremely well (though they do not generally outperform intra-domain transfer). We note that preliminary testing with grayscale ImageNet showed that this “color channel advantage” appears to be not solely responsible for the observed asymmetry, however.

Another implication of our results is that data domains possess very narrow definitions - judging by their performance, RadNet’s CT images are part of the same subdomain as the LiTS CT images, but not as the BraTS MRI images - if there exists such a thing as a medical image domain, its subdomains (CTs, MRIs, X-rays, etc.) are distinct entities divided by

generalization gaps. Depending on which two imaging modalities are compared, the gap has a different width, with CTs and X-rays possessing only a minute gap compared to CTs and MRIs. This result aligns perfectly with intuitive reasoning - CT and X-ray images operate on the same physics, attenuation of high-energy radiation, while MRI images are created via nuclear magnetic resonance.

Finally, we observe that an increase in the scale of available pretraining data almost universally improved transfer performance of RadNet-pretrained models, often even beyond ImageNet performance (cf. Figs. 2, 3).

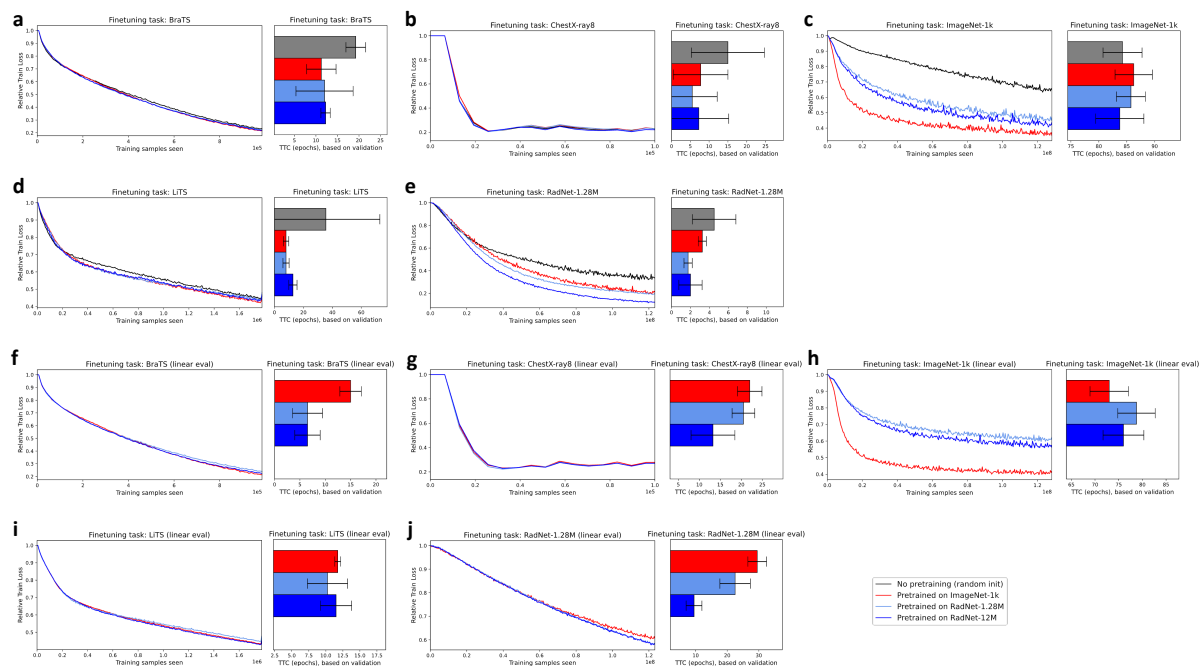


**Fig. 4: Training loss behavior and time to convergence are improved by intra-domain transfer.**

Training loss and time to convergence (based on a running mean of the validation performance) for each combination of pretraining dataset and finetuning task of experiments 1 and 2 are on display: **a**, Finetuning on BraTS2020. **b**, Finetuning on ChestX-Ray8. **c**, Finetuning on ImageNet-1k. **d**, Finetuning on LiTS 2017. **e**, Finetuning on RadNet. **f**, Linear evaluation on BraTS2020. **g**, Linear evaluation on ChestX-Ray8. **h**, Linear evaluation on ImageNet-1k. **i**, Linear evaluation on LiTS 2017. **j**, Linear evaluation on RadNet.

#### **4.1 Additional feature space analysis**

Our second hypothesis can be further scrutinized by quantifying feature reuse - if ImageNet pretraining offers a feature set of above-average generalizability, we should observe increased feature reuse compared to other pretraining datasets. We also expect to see a higher feature reuse for the ImageNet→RadNet scenario compared to the RadNet→ImageNet scenario.

Figs. 5a-e depict such a quantification, approximating the representational similarity of lowest-level convolution filters before and after finetuning using Centered Kernel Alignment [25] (RBF-CKA). We find that feature reuse is indeed greater in intra-domain than in cross-domain transfer scenarios for the ImageNet and RadNet classification tasks, but not for the LiTS segmentation task. Similarly to our observations on performance, reduced feature reuse reaffirms that CT images and MRI images constitute separate data domains. Additionally, we

observe the expected higher average feature reuse for ImageNet pretraining (averaged across all scenarios), compared to RadNet pretraining or no pretraining (cf. Fig. 5f). Interestingly, this feature reuse remains high even when the color channels no longer encode color, e.g. in CT images, or encode different information, like MRI sequences. The implication is that for early convolution kernels, ImageNet-pretraining encodes shape and texture much more strongly than color. This is in agreement both with our previous observations, as well as literature [26].

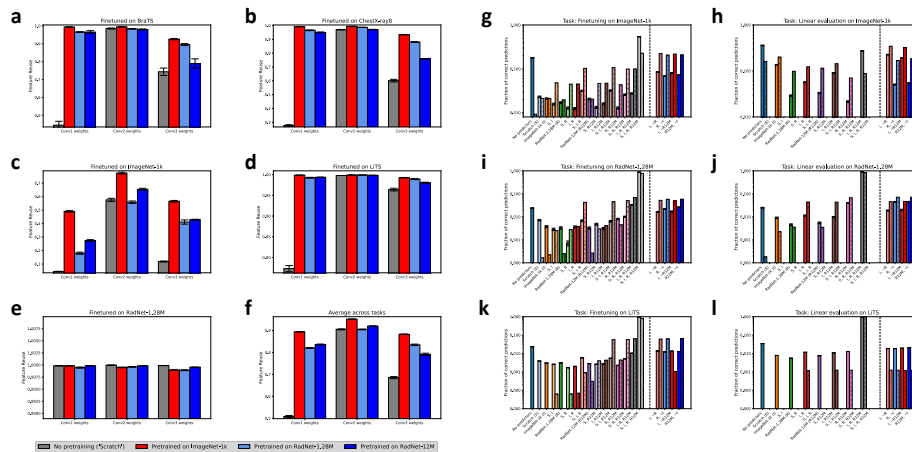


**Fig. 5: Intra-domain transfer leads to development of unique features and meaningful feature reuse.**

Increased feature reuse is evident for intra-domain transfer scenarios. Feature reuse is measured for the first three convolution layers of the pretrained and finetuned models (using RBF-kernel CKA). Feature reuse is shown for: **a**, Finetuning on BraTS2020. **b**, Finetuning on ChestX-Ray8. **c**, Finetuning on ImageNet-1k. **d**, Finetuning on LiTS 2017. **e**, Finetuning on RadNet. **f**, Average feature reuse across all tasks in experiment 1. Subfigures **g-l** encode what fraction of the dataset was correctly predicted by which pretraining sources (i.e. the bar labeled “ImageNet” shows the fraction of the test set identified correctly only by the ImageNet-pretrained model, but not by any other models). This was done for: **g**, Finetuning on ImageNet-1k. **h**, Linear evaluation on ImageNet-1k. **i**, Finetuning on RadNet-1.28M. **j**, Linear evaluation on RadNet-1.28M. **k**, Finetuning on LiTS 2017. **l**, Linear evaluation on LiTS 2017. An intra-domain advantage exists, with a significant number of data points only predicted by the model pretrained on data of the same domain. This effect is amplified in the linear evaluation scenario.

## **4.2 The nature of the intra-domain transfer performance gains**

To understand where the performance gains of RadNet pretraining are found in practical terms, we investigated two possibilities: I) Unique low-level features which models acquire during in-domain pretraining are responsible for the intra-domain advantage. In this case we expect to see many data points which only the model with the intra-domain advantage correctly identifies and few or no data points which only the other models correctly identify. II) Alternatively, the classification process could be so intractable that such features cannot be isolated. In that case, whether or not a data point is correctly identified by a model should appear close to random, depending only on that model’s known performance but not the data point itself.

Figs. 5g-l display histograms of the fraction of data points (images in classification, pixels in segmentation) correctly identified by the combination of models described on the X-axis. For example, the bar labeled “ImageNet” shows the number of data points identified correctly only by the ImageNet-pretrained model, but not by any other models. The corresponding hatched bars show the expected numbers for the same combination of models, assuming the second explanation is correct.

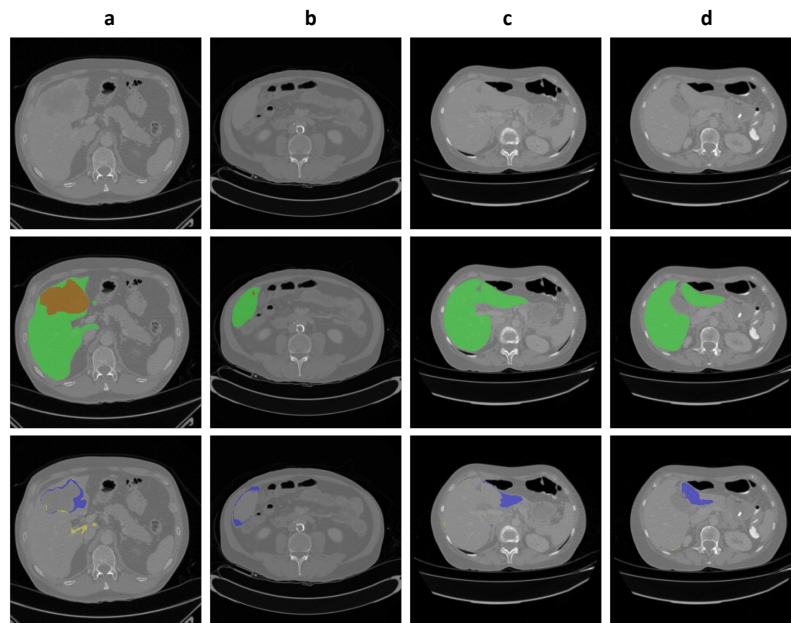


**Fig. 6: RadNet’s intra-domain advantage relates to explainable, macroscopic image properties.**

Four example images from the LiTS 2017 segmentation task are shown, containing, from top to bottom, the original image, the ground truth segmentations (green for liver tissue, red for lesions), and areas correctly predicted only by the RadNet-pretrained model, but not the ImageNet-pretrained model (blue) and the reverse case (yellow). Each image corresponds to one or two of the three typical scenarios in which RadNet appears to outperform ImageNet: **a**, Border region between liver and tumor. **b**, Border region between liver and surrounding tissue. **c**, Semi-insular region of the liver. **d**, Insular region of the liver. Note that the images shown are some of the more extreme examples - most of the time, the differences in predictions are much more minute.

We observe that two models with similar performance do not necessarily correctly classify the same data. Similarly, models with superior performance do not correctly classify a strict superset of data compared to models of inferior performance. This observation is in agreement with previous observations by Cohen et al. [7]. While there exists for every model at least a small number of data points which only that model could correctly identify, this number is always highest for the model(s) pretrained on the task domain (rightmost bars in Figs. 5g-l). This effect is again substantially magnified during linear evaluation. From these observations and the significant difference between the hatched and unhatched bars, we conclude that explanation I) is true. Interestingly, not all of the unique features or feature combinations hypothesized by explanation I) are learned by any one model, with notably different predictions even between RadNet-1.28M and RadNet-12M pretraining.

Through investigation of around 60 LiTS images with high prediction discrepancies between RadNet- and ImageNet-pretrained models, we found that an appreciable part of the performance gains for the LiTS liver segmentation corresponded to explainable, macroscopic

image/region properties. Most improvements are observed in border regions between two classes and for (semi-)insular segmentation targets like seemingly unconnected pieces of liver tissue, whose connection to the liver is vertical. All three scenarios seem reasonable for RadNet-pretrained models to perform well in: Insular areas of organ tissue are highly likely to appear in the training set during RadNet-pretraining and unlikely during ImageNet-pretraining. Furthermore, contrast-enhancing features must be learned during RadNet pretraining to identify structures, whereas ImageNet-pretraining can do the same using only texture or color information, giving RadNet-pretrained models a distinct advantage in tissue border regions on the colorless CT images of LiTS or RadNet, where the unenhanced contrast is low. Fig. 6 shows several representative examples of this advantage for RadNet- vs. ImageNet-pretraining in the “LiTS, linear evaluation” scenario.

## **5 Conclusions & Outlook**

In this paper, we systematically explored the efficacy of self-supervised pretraining and transfer learning across multiple datasets from the natural and medical image domains. Our experiments demonstrated the existence of a performance-degrading generalization gap that occurs during transfer learning if the pretraining and finetuning dataset originate from different domains. They further highlighted that different combinations of pretraining and finetuning datasets yield differently sized gaps, depending on task domain, complexity, and whether linear evaluation was performed. We confirmed our initial hypotheses that I) intra-domain pretraining is generally preferable, even though II) some datasets such as ImageNet generalize better on average. Finally, we provided evidence that in-domain pretraining yields unique low-level features which are preserved during finetuning on data from the same domain, and discussed the nature of the performance gains they provided.

Several limitations apply to this work. Firstly, our conclusions may not generalize to different hyperparameters. Models trained using pretraining algorithms, supervision levels, or data domains different from ours may not support our conclusions. The generalization gap asymmetry might not be a product of intrinsic data domain characteristics, but rather of the complexity of the downstream task - while RadNet-1.28M has the same size as ImageNet-1k, a task of the same complexity (1000 unique and mutually exclusive classes vs. 6) is almost impossible to achieve using automatically labeled, generic CT scans. However, this limitation is only of theoretical concern, as all practical tasks in image-guided medical machine learning come with this caveat.

We summarize a general set of rules for optimal transfer learning performance, based on our experiments:

- Intra-domain transfer learning typically outperforms cross-domain transfer learning by at least a small margin in performance. Occasionally, this is accompanied by increased convergence speed. In short, **“My medical AI should be looking at pictures of tumors instead of birds to learn about tumors.”**
- The higher the downstream task’s complexity, the more valuable intra-domain pretraining becomes.
- Large-scale pretraining almost always results in performance gains. We observed no performance saturation for further upscaling of the pretraining in many scenarios, with RadNet-12M-pretrained models often outperforming ImageNet-1k-pretrained models.

This insight is particularly relevant for clinical settings, where plentiful data from the same imaging modality are often available but very costly to annotate. **This data should be leveraged in unsupervised pretraining where possible.**

- **There is no “one size fits all” solution.** Using ImageNet as a default pretraining dataset is suitable. However, if the best possible performance on that task is more relevant than a quick solution, there is no substitute for testing multiple pretraining datasets, particularly from the same data domain as the task.
- We observed that the generalization gap varies very nuancedly; Even the target class or metric, e.g. liver vs. lesion on the LiTS task, can be relevant for the choice of pretraining dataset.

In future work, we plan to extend RadNet-12M with additional data from other modalities, such as MRI and X-rays. We also plan to pretrain additional architectures using RadNet and publish their model weights. Further, we believe that research extending our work to other pretraining algorithms and supervised scenarios constitutes a promising research direction, which would address some of the limitations of this work. Creating large-scale models pretrained on a previously untapped wealth of unlabeled clinical images will be of great value to the exponentially growing, yet notoriously data-starved [27] field of medical computer vision.

## References

- [1] M. Cherti and J. Jitsev, "Effect of pre-training scale on intra- and inter-domain, full and few-shot transfer learning for natural and X-Ray chest images," in *2022 International Joint Conference on Neural Networks (IJCNN)*, Padua, Italy: IEEE, Jul. 2022, pp. 1–9. doi: 10.1109/IJCNN55064.2022.9892393.
- [2] J. Deng, W. Dong, R. Socher, L.-J. Li, Kai Li, and Li Fei-Fei, "ImageNet: A large-scale hierarchical image database," in *2009 IEEE Conference on Computer Vision and Pattern Recognition*, Miami, FL: IEEE, Jun. 2009, pp. 248–255. doi: 10.1109/CVPR.2009.5206848.
- [3] F. C. Ghesu *et al.*, "Contrastive self-supervised learning from 100 million medical images with optional supervision," *J. Med. Imag.*, vol. 9, no. 06, Nov. 2022, doi: 10.1117/1.JMI.9.6.064503.
- [4] X. Mei *et al.*, "RadImageNet: An Open Radiologic Deep Learning Research Dataset for Effective Transfer Learning," *Radiology: Artificial Intelligence*, vol. 4, no. 5, p. e210315, Sep. 2022, doi: 10.1148/ryai.210315.
- [5] M. Raghu, C. Zhang, J. Kleinberg, and S. Bengio, "Transfusion: Understanding Transfer Learning for Medical Imaging," in *Advances in Neural Information Processing Systems*, H. Wallach, H. Larochelle, A. Beygelzimer, F. d'Alché-Buc, E. Fox, and R. Garnett, Eds., Curran Associates, Inc., 2019. [Online]. Available: <https://proceedings.neurips.cc/paper/2019/file/eb1e78328c46506b46a4ac4a1e378b91-Paper.pdf>
- [6] A. Newell and J. Deng, "How Useful Is Self-Supervised Pretraining for Visual Tasks?," in *2020 IEEE/CVF Conference on Computer Vision and Pattern Recognition (CVPR)*, Seattle, WA, USA: IEEE, Jun. 2020, pp. 7343–7352. doi: 10.1109/CVPR42600.2020.00737.
- [7] J. P. Cohen, M. Hashir, R. Brooks, and H. Bertrand, "On the limits of cross-domain generalization in automated X-ray prediction," in *Proceedings of the Third Conference on Medical Imaging with Deep Learning*, T. Arbel, I. Ben Ayed, M. de Bruijne, M. Descoteaux, H. Lombaert, and C. Pal, Eds., in *Proceedings of Machine Learning Research*, vol. 121. PMLR, Jul. 2020, pp. 136–155. [Online]. Available: <https://proceedings.mlr.press/v121/cohen20a.html>
- [8] S. Gururangan *et al.*, "Don't Stop Pretraining: Adapt Language Models to Domains and Tasks," in *Proceedings of the 58th Annual Meeting of the Association for Computational Linguistics*, Online: Association for Computational Linguistics, 2020, pp. 8342–8360. doi: 10.18653/v1/2020.acl-main.740.
- [9] H. Petzka, M. Kamp, L. Adilova, C. Sminchisescu, and M. Boley, "Relative flatness and generalization," in *Advances in Neural Information Processing Systems*, 2021, pp. 18420–18432.
- [10] S. Ben-David, J. Blitzer, K. Crammer, and F. Pereira, "Analysis of Representations for Domain Adaptation," in *Advances in Neural Information Processing Systems*, B. Schölkopf, J. Platt, and T. Hoffman, Eds., MIT Press, 2006. [Online]. Available: [https://proceedings.neurips.cc/paper\\_files/paper/2006/file/b1b0432ceafb0ce714426e9114852ac7-Paper.pdf](https://proceedings.neurips.cc/paper_files/paper/2006/file/b1b0432ceafb0ce714426e9114852ac7-Paper.pdf)
- [11] Y. Mansour, M. Mohri, and A. Rostamizadeh, "Domain Adaptation: Learning Bounds and Algorithms," in *Proceedings of The 22nd Annual Conference on Learning Theory (COLT 2009)*, Montréal, Canada, 2009. [Online]. Available: <http://www.cs.nyu.edu/~mohri/postscript/nadap.pdf>
- [12] P. Bilic *et al.*, "The Liver Tumor Segmentation Benchmark (LiTS)," *Medical Image Analysis*, vol. 84, p. 102680, Feb. 2023, doi: 10.1016/j.media.2022.102680.
- [13] R. Mehta *et al.*, "QU-BraTS: MICCAI BraTS 2020 Challenge on Quantifying Uncertainty in Brain Tumor Segmentation – Analysis of Ranking Scores and Benchmarking Results," *Melba*, vol. 1, no. August 2022, pp. 1–54, Aug. 2022, doi: 10.59275/j.melba.2022-354b.

- [14] X. Wang, Y. Peng, L. Lu, Z. Lu, M. Bagheri, and R. M. Summers, "ChestX-Ray8: Hospital-Scale Chest X-Ray Database and Benchmarks on Weakly-Supervised Classification and Localization of Common Thorax Diseases," in *2017 IEEE Conference on Computer Vision and Pattern Recognition (CVPR)*, Honolulu, HI: IEEE, Jul. 2017, pp. 3462–3471. doi: 10.1109/CVPR.2017.369.
- [15] S. Koitka, L. Kroll, E. Malamutmann, A. Oezcelik, and F. Nensa, "Fully automated body composition analysis in routine CT imaging using 3D semantic segmentation convolutional neural networks," *European Radiology*, vol. 31, no. 4, pp. 1795–1804, Apr. 2021, doi: 10.1007/s00330-020-07147-3.
- [16] F. Jonske *et al.*, "Deep Learning–driven classification of external DICOM studies for PACS archiving," *European Radiology*, vol. 32, no. 12, pp. 8769–8776, Dec. 2022, doi: 10.1007/s00330-022-08926-w.
- [17] T. Chen, S. Kornblith, M. Norouzi, and G. Hinton, "A Simple Framework for Contrastive Learning of Visual Representations," in *Proceedings of the 37th International Conference on Machine Learning*, H. D. III and A. Singh, Eds., in Proceedings of Machine Learning Research, vol. 119. PMLR, Jul. 2020, pp. 1597–1607. [Online]. Available: <https://proceedings.mlr.press/v119/chen20j.html>
- [18] K. He, X. Zhang, S. Ren, and J. Sun, "Deep Residual Learning for Image Recognition," in *2016 IEEE Conference on Computer Vision and Pattern Recognition (CVPR)*, Las Vegas, NV, USA: IEEE, Jun. 2016, pp. 770–778. doi: 10.1109/CVPR.2016.90.
- [19] Y. You, I. Gitman, and B. Ginsburg, "Large Batch Training of Convolutional Networks," 2017, doi: 10.48550/ARXIV.1708.03888.
- [20] H. Zhang *et al.*, "Context Encoding for Semantic Segmentation," in *2018 IEEE/CVF Conference on Computer Vision and Pattern Recognition*, IEEE, 2018, pp. 7151–7160.
- [21] Sergey Ioffe and Christian Szegedy, "Batch Normalization: Accelerating Deep Network Training by Reducing Internal Covariate Shift," in *Proceedings of the 32nd International Conference on Machine Learning*, Francis Bach and David Blei, Eds., PMLR, Jun. 2015, pp. 448–456. [Online]. Available: <https://proceedings.mlr.press/v37/ioffe15.html>
- [22] O. Ronneberger, P. Fischer, and T. Brox, "U-Net: Convolutional Networks for Biomedical Image Segmentation," in *Medical Image Computing and Computer-Assisted Intervention – MICCAI 2015*, N. Navab, J. Hornegger, W. M. Wells, and A. F. Frangi, Eds., in Lecture Notes in Computer Science, vol. 9351. Cham: Springer International Publishing, 2015, pp. 234–241. doi: 10.1007/978-3-319-24574-4\_28.
- [23] A. Paszke *et al.*, "PyTorch: An Imperative Style, High-Performance Deep Learning Library," in *Advances in Neural Information Processing Systems*, H. Wallach, H. Larochelle, A. Beygelzimer, F. d'Alché-Buc, E. Fox, and R. Garnett, Eds., Curran Associates, Inc., 2019. [Online]. Available: [https://proceedings.neurips.cc/paper\\_files/paper/2019/file/bdbca288fee7f92f2bfa9f7012727740-Paper.pdf](https://proceedings.neurips.cc/paper_files/paper/2019/file/bdbca288fee7f92f2bfa9f7012727740-Paper.pdf)
- [24] B. L. Welch, "The Generalization of 'Student's' Problem when Several Different Population Variances are Involved," *Biometrika*, vol. 34, no. 1–2, pp. 28–35, 1947, doi: 10.1093/biomet/34.1-2.28.
- [25] S. Kornblith, M. Norouzi, H. Lee, and G. Hinton, "Similarity of Neural Network Representations Revisited," in *Proceedings of the 36th International Conference on Machine Learning*, K. Chaudhuri and R. Salakhutdinov, Eds., in Proceedings of Machine Learning Research, vol. 97. PMLR, Jun. 2019, pp. 3519–3529. [Online]. Available: <https://proceedings.mlr.press/v97/kornblith19a.html>
- [26] R. Geirhos, P. Rubisch, C. Michaelis, M. Bethge, F. A. Wichmann, and W. Brendel, "ImageNet-trained CNNs are biased towards texture; increasing shape bias improves accuracy and robustness.," in *International Conference on Learning Representations*, 2019. [Online]. Available: <https://openreview.net/forum?id=Bygh9j09KX>
- [27] J. Egger *et al.*, "Medical deep learning—A systematic meta-review," *Computer Methods and Programs in Biomedicine*, vol. 221, p. 106874, 2022, doi: <https://doi.org/10.1016/j.cmpb.2022.106874>.



- [28] Python Software Foundation, “Python gzip package,” Jun. 11, 2023. <https://docs.python.org/3/library/gzip.html> (accessed Jun. 12, 2023).
- [29] C. E. Shannon, “A Mathematical Theory of Communication,” *Bell System Technical Journal*, vol. 27, no. 3, pp. 379–423, Jul. 1948, doi: 10.1002/j.1538-7305.1948.tb01338.x.
- [30] I. Loshchilov and F. Hutter, “Decoupled Weight Decay Regularization,” 2017, doi: 10.48550/ARXIV.1711.05101.

## **Acknowledgements**

We acknowledge CAMed (COMET K-Project 871132), enFaced (FWF KLI 678), enFaced 2.0 (FWF KLI 1044) and KITE (Plattform für KI-Translation Essen) from the REACT-EU initiative (EFRE-0801977, <https://kite.ikim.nrw/>)

## **Code availability**

The pretraining and finetuning code framework developed for this paper, including configuration files, code used to create figures, and results logs can be found at <https://github.com/TIO-IKIM/Transfer-learning-across-domain-boundaries>. Our code, and some publicly available code we build on, are subject to the MIT license. For publicly available datasets, we link the datasets and provide our data layout/splits.

## **Data availability**

We link the sources of the public datasets we used in our code repository. The RadNet datasets are not made public. All pretrained/finetuned models reported are linked on <https://github.com/TIO-IKIM/Transfer-learning-across-domain-boundaries> and may be used for further research. This permission includes models pretrained on the RadNet datasets.

## **Additional notes**

This paper is a preprint, and the results presented are therefore subject to change, addition of content, or restructuring according to the submission guidelines of the eventual publication journal.

# Supplementary Materials

## S1 - Significance of experimental results

We report the significance of performance gains or losses based on Welch's t-test. This test quantifies the probability that two populations of samples with different mean and standard deviation were sampled from the same underlying distribution. In layman's terms, the resulting p-value is the probability that our performance gain comes from a real effect in the experiment and is not random noise. Figs. SF1-3 contain the relative performance gains/losses between any pairing of pretraining options on a specific finetuning task and their corresponding p-value. Note that the p-values for the LB/UB-adjusted RadNet results generally have increased uncertainties compared to the unadjusted results. This additional uncertainty stems from the interpolation process and error propagation, and does not imply any sort of training instability for RadNet-pretrained models.

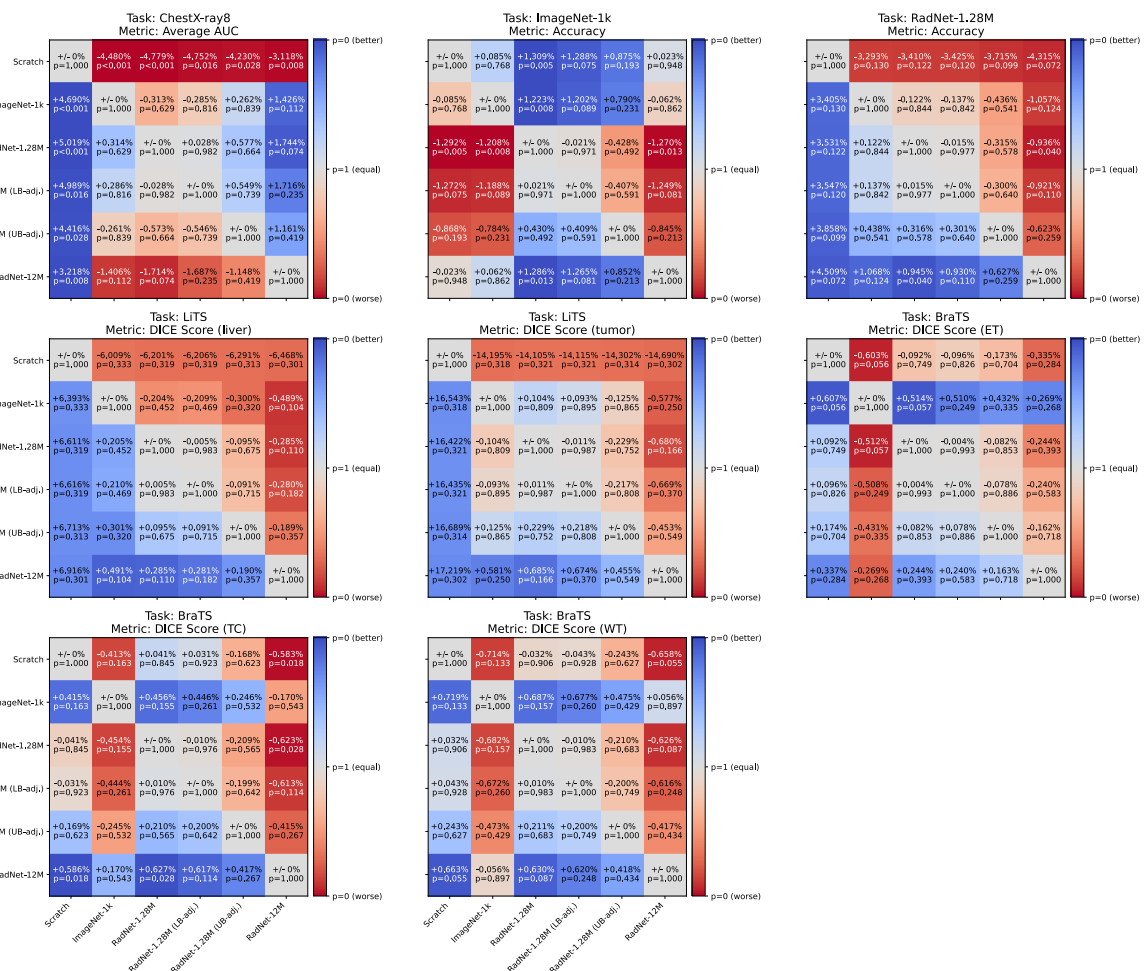


**Fig. SF1: Relative performance and significance of results in experiment 1.**

In each subplot, each possible pair of pretraining options is compared once for the task and performance metric specific to that subplot. The p-values are derived from Welch's t-test. To read a subplot, apply the following logic: For the given task and metric, pretraining on the dataset in this row is better/worse than pretraining on the dataset in this column by some percentage and with a significance of the given p-value.

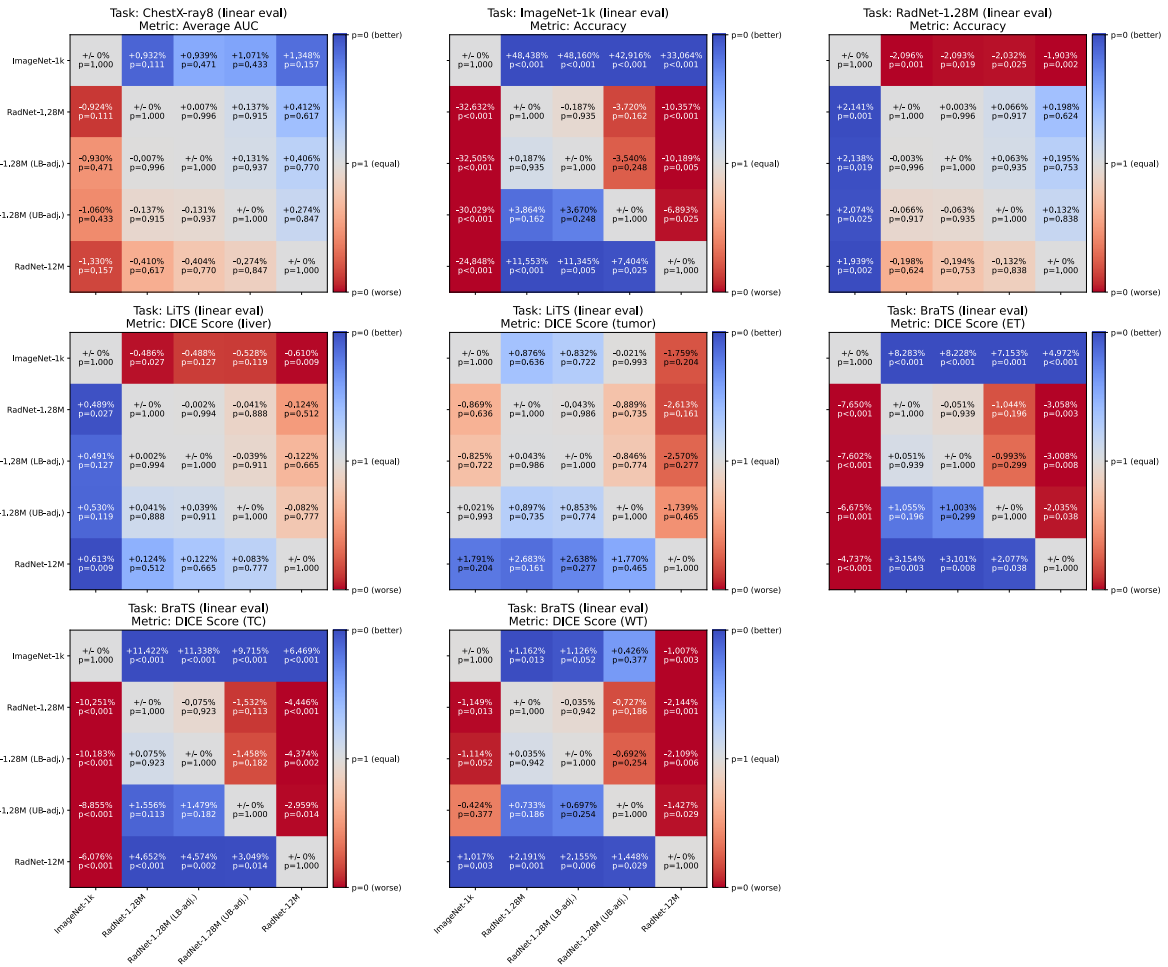


**Fig. SF2: Relative performance and significance of results in experiment 2.**

In each subplot, each possible pair of pretraining options is compared once for the task and performance metric specific to that subplot. The p-values are derived from Welch's t-test. To read a subplot, apply the following logic: For the given task and metric, pretraining on the dataset in this row is better/worse than pretraining on the dataset in this column by some percentage and with a significance of the given p-value.

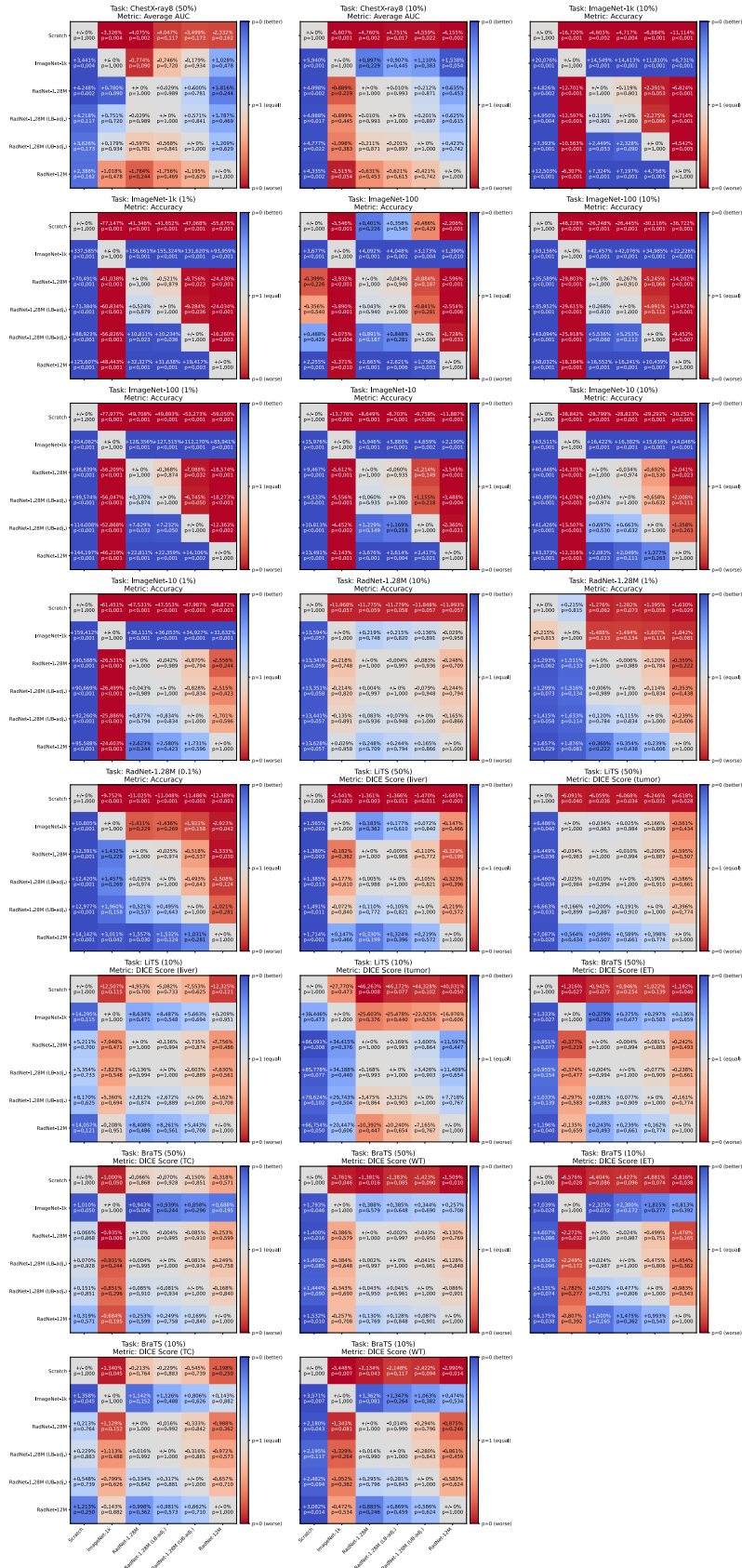


**Fig. SF3: Relative performance and significance of results in experiment 3.**

In each subplot, each possible pair of pretraining options is compared once for the task and performance metric specific to that subplot. The p-values are derived from Welch's t-test. To read a subplot, apply the following logic: For the given task and metric, pretraining on the dataset in this row is better/worse than pretraining on the dataset in this column by some percentage and with a significance of the given p-value.

## **S2 - On hyperparameter choice**

One can make a fair comparison between two pretraining datasets in two ways - either one argues that both competing training procedures are maximally optimized (which cannot be guaranteed without an exhaustive hyperparameter search) and therefore represent the best outcome the training procedure can offer. In this case, hyperparameters for networks pretrained on different data may be different on the same downstream task, if those parameters really do squeeze out that extra .1 percent of accuracy.

Alternatively, one can argue that both competing training procedures are not optimized, using arbitrary hyperparameters that converge with a reasonable performance when training from scratch and which are constant for any given downstream task. However, this may favor one of the competitors (which one specifically is unclear). Whether it actually does is impossible to know without a sufficiently fine-grained mapping of the entire hyperparameter space.

Given the prohibitive computational cost of such endeavors, we opt to not perform any large hyperparameter searches, and instead make an arbitrary (but sufficiently stable and performant) choice of hyperparameters for each downstream task's finetuning process, creating as fair a comparison as possible, by first testing each task with a few learning rates and decay factors on an untrained model and then reusing that parameter set.

Performance metrics reported in this paper may fall short of literature equivalents where such a hyperparameter search or extensive auxiliary procedures (additional regularization, auxiliary heads, optimizer choice, complex learning rate scheduling, etc.) were performed by the authors (although they remain surprisingly competitive on some tasks, considering this handicap). We abstain from using pre-existing hyperparameter heuristics or auxiliary procedures where possible, as those were typically developed by observing effectiveness in a specific domain (usually ImageNet). One exception to this approach is the use of the square root learning rate heuristic for LARS [17] and on ImageNet, as optimization using LARS was necessary to reduce the computation time requirements to within reasonable time scales. The hyperparameters for all runs can be found in Tab. ST1 or at <https://github.com/TIO-IKIM/Transfer-learning-across-domain-boundaries>

It is important to note that while the comparisons presented in our experiments are fair in the sense of unbiased sampling of the hyperparameter space, they are just that; a sample in a very high-dimensional space. It is therefore possible that the behavior we report is different in other areas of this parameter space and that the conclusions we draw do not generalize, although preliminary experiments with other parameters do not suggest that this is the case. Similarly, our results depend on the available data and a varied dataset with more medical imaging modalities or more data may produce different results. The scale of our experiments implies that neither is the case, but does not guarantee it.

## **S3 - Correlation between neighboring slices in RadNet**

Neighboring slices of one CT image are necessarily similar, since (thankfully) organs cannot have random gaps or slices offset in random directions. Hence, already having neighboring slices in the dataset reduces the new information a slice added to the dataset can provide during training. To some degree, this is unavoidable, because human anatomy is a strongly

constraining factor. However, even compared to a dataset in which every slice comes from the CT scan of a different, random patient, some information is redundant. While we cannot provide a dataset consisting completely of uncorrelated slices, we can scale up our initial dataset until the information content of the new dataset is the same as that of an entirely uncorrelated dataset the size of our initial dataset, so that only the domain-specific redundancy remains.

We will try to motivate an approximate lower and upper bound for a scale factor  $S$ , by which the amount of data in RadNet-1.28M should be multiplied to achieve a fairer comparison. In our results, we report the performances of a hypothetical RadNet-1.28M scaled with the lower and upper bound for  $S$ . These performances are estimated using interpolation.

To arrive at an approximate lower bound  $S_{LB}$ , we test the compressibility of a set of correlated images (i.e. an entire 3D CT scan) compared to an equally-sized set of random images drawn from RadNet. Any gain in compressibility is most likely due to the exploitation of correlated image features, implying a reduced information content in the correlated images. This calculation yields a lower bound because the compression algorithm is not guaranteed to be able to exploit every correlation - in practice,  $S$  is likely to be much larger. To measure compressibility, we used Python’s gzip compression package [28] (at default settings). We calculate the compressibility ratio across all images (weighted by the number of slices) in RadNet-1.28M and find:  $S_{LB} = \sum_{i=1}^{90663} \frac{c_{corr.(i)}}{c_{random}} w_i \approx 1.136$ .

To arrive at an upper bound  $S_{UB}$ , we utilize the concept of mutual information (MI) [29].  $MI$  quantifies the amount of information about a variable  $X_1$  which can be inferred by observing a correlated variable  $X_2$ . Note that  $MI$  does not specifically capture representational similarity in the way a human observer might understand, only a mathematical measure of “shared information” (unlike CKA which was expressly designed for the former purpose).

For every combination of an image and a random reference image, we can establish a relative  $MI$  between two slices of the former image as follows:

- Calculate the  $MI$  between every combination of two image slices of the first image (In theory, this can be done for all combinations, but beyond around 10 slices, the  $MI$  will already be quite small)
- Normalize these  $MI$  values by using the  $MI$  between a slice and itself as  $MI_{max}$  and the average  $MI$  between the image slice and slices from the reference image as  $MI_{min}$ . The resulting relative utility value  $U$ , with  $U_{i,j} = 1 - \frac{MI_{i,j} - MI_{min}}{MI_{max} - MI_{min}}$ , is a measure of the usefulness of a slice, compared to a random one. The closer  $U_{i,j}$  is to 0, the less new information that slice will give us. A utility of 0 indicates that a slice with an identical distribution (in a 2d-histogram) already exists in our data, while a 1 indicates that the new slice is as new as a slice from a random reference image.

We can then calculate our upper bound  $S_{UB}$  as the sum of the worst utility  $U_{i,max}$  for every slice  $i$ , divided by the number of slices in our dataset. In order not to “count double”, slices are added to the dataset one by one, calculating the worst utility with respect to the dataset at the time that the new image is added.

Our calculation yields an upper bound because the average  $MI$  between slices of the same CT image is likely, albeit not guaranteed, to stem from anatomy-related correlation (since we have already subtracted the average  $MI$  that we expect to exist between two slices of different CT images, which should cover aspects all CT images have in common, like the bed or air around the patient). For RadNet-1.28M, we find that  $S_{UB} \approx 3.807$ .

A typical distribution of  $U$  vs. frame distance (for all slice pairings in a single image and a reference image) is shown in Fig. SF4. Note that this distribution varies from image to image depending on reference image, captured body region, filters, and frame distance.

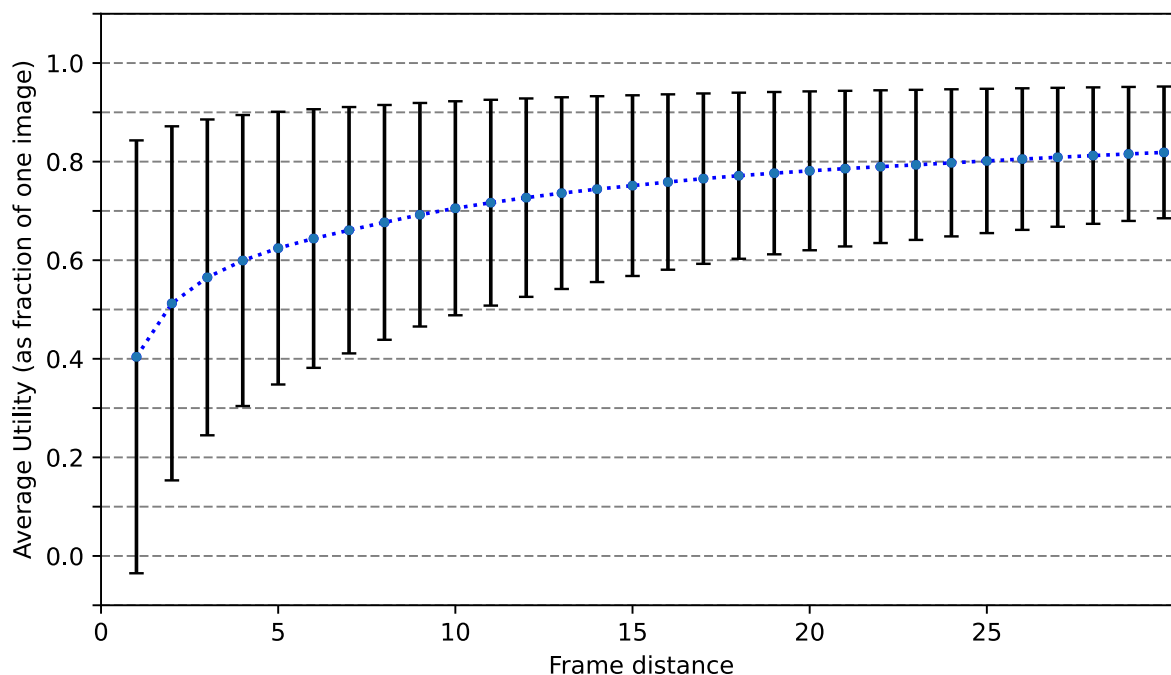


**Fig. SF4: Typical distribution of image utility in a single 3D CT scan.**

In a 3D CT scan, the closer an image slice is to its neighbor, the more information it contains about its neighbor. As seen in this figure, the actual value of an image is significantly decreased if its direct neighbor is already in the dataset. The curve shown was computed for a CT with a frame distance of 5mm. Its shape is representative for most scans, although scan region, frame distance, and image quality cause significant variations.

Note that the upper bound represents a more realistic approximation of  $S$ : The underlying 2d-histograms of the  $MI$  calculation are very finely binned (64 bins wide along both axes vs. 4096 possible integer values each pixel can have in a typical CT), which implies that high  $MI$  values do indeed represent highly similar images and not just vaguely similar histograms, while the lower bound is somewhat restricted in how high it can go because of things like noise (which is incompressible) and imperfect compression of existing similarities.

#### **S4 - Feature Uniqueness**

By randomly splitting all features of a convolution layer into smaller segments and averaging over the CKA similarity of all pairings, we can obtain a measure for the uniqueness of the features obtained during pretraining (cf. Fig. SF5). Surprisingly, we find that RadNet-based pretraining yields substantially greater feature uniqueness than ImageNet-based pretraining, in spite of working without any color information. A possible explanation for this phenomenon

is two-fold: Firstly, given a number of (as established above) correlated images, a part of the features created will likely be the result of overfitting to the differences between two or more highly correlated images. These features, representative of statistical noise, will be highly unique, but not useful. This explanation is corroborated by the fact that the RadNet-1.28M-pretrained model has more unique features than the RadNet-12M-pretrained model. Secondly, as ImageNet pretraining encodes color information, the feature uniqueness of its respective model may be reduced if the model encodes the same shape, texture, or gradient multiple times in different color combinations, which it may have to do in some cases during pretraining. This would explain why ImageNet-1k encodes less unique features than both RadNet-pretrained models.

Between the increased feature uniqueness, and favorable performance in intra-domain transfer scenarios, we conclude that RadNet-based pretraining results in a number of highly specialized features, which increase performance on CT-based downstream tasks.

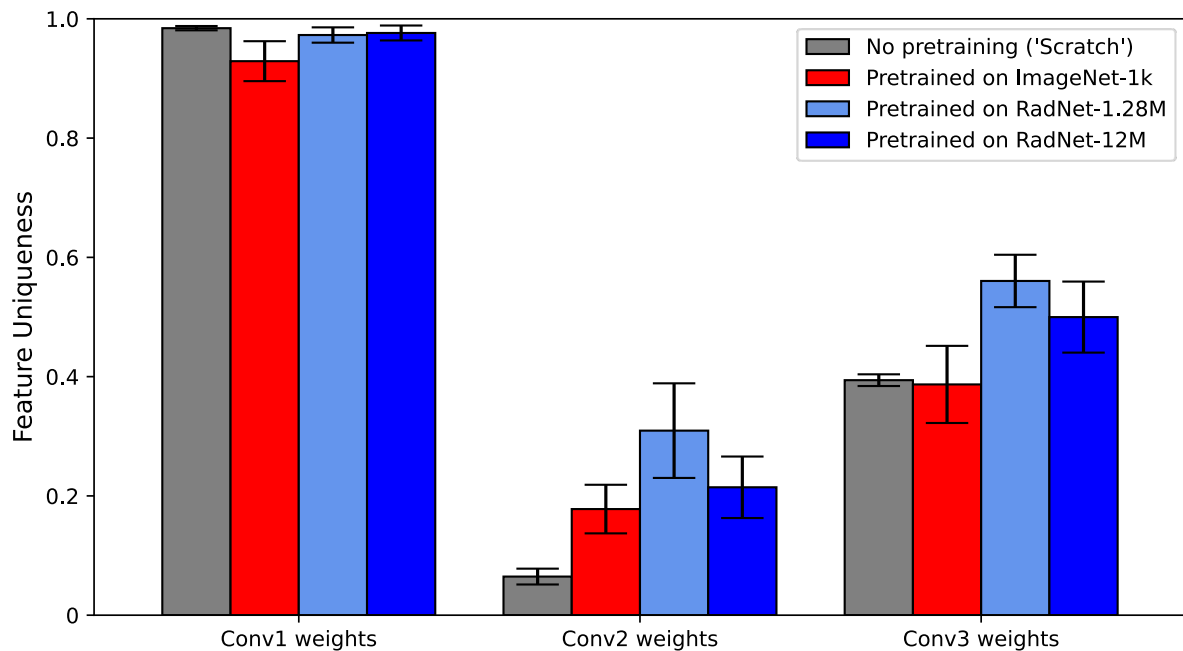


**Fig. SF5: Feature uniqueness of convolution layers after pretraining.**

For each model, feature uniqueness is quantified by comparing the similarity of the convolution kernels after pretraining with themselves, by way of splitting the set of all kernels of a convolution layer into subsets and comparing each individual pairing. The higher the uniqueness coefficient, the more the individual kernels differ from one another. Surprisingly, RadNet-pretrained models appear to have more unique features than the ImageNet-pretrained model.



## Tables

Dataset name (pretraining)	Batch size	Learning rate	Optimizer	Method	# of images
ImageNet-1k	4096	4.8	LARS	SimCLR	1,281,167
RadNet-1.28M	4096	4.8	LARS	SimCLR	1,281,167
RadNet-12M	4096	4.8	LARS	SimCLR	12,034,617
Task name (Experiments 1, 2, 4)	Batch size	Learning rate	Optimizer	Decay factor	Class weights
BraTS 2020	128	1.0e-3	AdamW [30]	0.95	Background: 1 Others: 5
ChestX-Ray8	128	5.0e-4	AdamW	0.97	BG: 1e-3 Others: 1
ImageNet-1k	4096	4.8	LARS	0.97	Equal
LiTS 2017	128	2.0e-4	AdamW	0.97	BG: 1 Liver: 3 Lesion: 10
RadNet-1.28M	4096	1.0e-2 <sup>†</sup>	LARS	0.97	Equal
Task name (Experiment 3)	Batch size	Learning rate	Optimizer	Decay factor	Class weights
BraTS 2020 (M)	128	1.0e-3	AdamW	0.95	BG: 1 Others: 5
BraTS 2020 (S)	128	1.0e-3	AdamW	0.95	BG: 1 Others: 5
ChestX-Ray8 (M)	128	5.0e-4	AdamW	0.97	BG: 1e-3 Others: 1
ChestX-Ray8 (S)	128	5.0e-4	AdamW	0.97	BG: 1e-3 Others: 1
ImageNet-1k (S)	1024	2.4	LARS	0.97	Equal
ImageNet-1k (XS)	256	1.0e-4	AdamW	0.97	Equal
ImageNet-100	1024	2.4	LARS	0.97	Equal
ImageNet-100 (S)	256	1.0e-4	AdamW	0.97	Equal
ImageNet-100 (XS)	256	1.0e-4	AdamW	0.97	Equal
ImageNet-10	256	1.0e-4	AdamW	0.97	Equal
ImageNet-10 (S)	256	1.0e-4	AdamW	0.97	Equal

ImageNet-10 (XS)	64	1.0e-4	AdamW	0.97	Equal
LiTS 2017 (M)	128	2.0e-4	AdamW	0.97	BG: 1 Liver: 3 Lesion: 10
LiTS 2017 (S)	128	2.0e-4	AdamW	0.97	BG: 1 Liver: 3 Lesion: 10
RadNet (S)	1024	5.0e-3	LARS	0.97	Equal
RadNet (XS)	256	1.0e-4	AdamW	0.97	Equal
RadNet (XXS)	256	1.0e-4	AdamW	0.97	Equal

**Table ST1: Hyperparameters.**

Additional settings can be found in the config files at our code repository (<https://github.com/TIO-IKIM/Transfer-learning-across-domain-boundaries>). The “decay factor” entry refers to learning rate decay; all training runs used a decaying learning rate, where the learning rate would be reduced by multiplying with the decay factor after each epoch. ImageNet and RadNet finetuning tasks trained for 100 epochs, all other tasks for 50 epochs.

\* - Surprisingly, working with the usual batch size dependency for learning rates in LARS (which usually result in very large learning rates  $\geq 1$ ) caused significant instability and degraded performance in early experiments when finetuning on RadNet. Consequently, we reduced the learning rate until this behavior disappeared.